Application of a one-dimensional fuel-oil dilution model coupled with an empirical droplet-to-film formation strategy for predicting in-cylinder oil effects in a direct injection engine

Application of a one-dimensional fuel-oil dilution model coupled with an empirical droplet-to-film formation strategy for predicting in-cylinder oil effects in a direct injection engine

E D Renzis[1], V Mariani[1], G M Bianchi[1], S Falfari[1] and G Cazzoli[1]

[1] Department of Industrial Engineering, University of Bologna, Alma Mater Studiorum, Italy

edoardo.derenzis2@unibo.it

Abstract. Nowadays climate change due to the unnatural increment of green-house effect is one of the most critical environmental issues. In this context, internal combustion engines are still a short - term valuable solution. This is made possible by the study and the development of synthetic or alternative fuels, such e - gasolines and hydrogen. In this context, direct injection is still the most adopted strategy to improve internal combustion engine efficiency. The installation of the injector on the cylinder head may lead to the impact of the fuel on the wall of the cylinder liner. This phenomenon causes lubricant oil dilution, possibly increasing particulate matter emission at low load and abnormal combustions, known as low - speed pre-ignitions, at high load. The present paper aims to evaluate the influence of a set of established key parameters anticipating the effects of lubricant oil - fuel diffusion through a one - dimensional model implemented in Python. The model accounts for the runtime deposition of the fuel film by means of the results of a three - dimensional Computational Fluid Dynamics spray simulation. The model accounts also for the heat and mass transfer between species and the liquid fuel phase change for a representative setup of nowadays injectors. The dilution of a multigrade lubricant oil caused by synthetic fuels under an engine cold start operative condition is evaluated in this work.

1. Introduction

The current environmental concern is leading to narrower regulations for pollutant emissions (particulate matter (PM), nitrogen oxides (NOx), unburned hydrocarbons (UHC), etc.) and for green - house gases (carbon dioxide (CO2)) in the field of light - duty vehicles. In this context, improved internal combustion engines (ICE) are still an affordable solution during the “green” transition of the current fleet. For this reason, in the last few decades manufacturers put efforts to develop new hardware and control strategies, while improving existing technologies to achieve cleaner and more efficient internal combustion engines (ICE). The most adopted solution is the coupling of engine turbocharging and downsizing with the direct injection, which positively affects the engine efficiency while ensuring the desired amount of power request. The joint application of engine downsizing and direct injection leads to a shorter time and path available for the fuel evaporation, thus enhancing the fuel walls impingement. With these regards, fuel impingement became a concerning issue also for gasoline engines and not only for diesel engines, which already adopted high pressure direct injection.

Fuel impingement is responsible for promoting diffusive combustion against premixed combustion, which contributes to particulate matter formation [1]. The generation of the wall film is influenced by different factors, such as the engine configuration (i.e. wall, spray, or air guided) [2], the injector location (center or side mounted injector), fuel properties (such as aromatic content, volatility and oxygen content) [3][4][5], injection system working parameters, for instance injection pressure and timing [6] and the wall temperature, which depends on the engine load. In particular, the cold start phase and low loads operating points have been heavily investigated since they are critical for particulate formation because at those conditions the engine walls are cold thus, the fuel impingement with film formation is more likely to occur [7]. The fuel impact on the liner wall has also the negative effects of contaminating and thickening the thin lubricant oil layer, which wets the liner. This contamination leads to the degradation of the lubricant oil viscosity and causes higher frictions, enhancing parts wear [8][9]. Besides, when the piston reaches the diluted film during the compression stroke, it scrapes part of the mixture which is carried into the piston top land crevice. At this point, due to the piston inertia, lubricant oil droplets may be scattered into the combustion chamber [10] and promote a diffusive combustion once the mixture is ignited or the droplets may ignite before the spark event can occur, causing the pre - ignition of the mixture [11][12]. In both cases, since lubricant oil is composed by hydrocarbons, its combustion leads to PM formation [13]. Also, in the work [14], the Authors conducted an experimental campaign employing a free – lubrication optical engine. Three different ways of feeding the lubricant oil and two fuel – injection modes were investigated to mimic the different ways by which the lubricant can reach the combustion chamber. In this way, it was possible to isolate the contribution of the lubricant oil in the particulate formation. Miller et Al. [15] studied the particulate emissions in a hydrogen powered internal combustion engine: the primary goal was to investigate the formation of combustion - generated particles derived from lubricant oil in the absence of fuel - produced soot. The study showed that diameter, number concentration and mass concentration of particles for all engine loading conditions were significantly smaller with respect to a diesel engine. Pfau et Al. [16] performed an experimental analysis by measuring the soot concentration in lubricant oil samples taken from a gasoline direct injection (GDI) engine: the results showed that the measured soot - in - oil levels were comparable to those in diesel engines. Uy et Al. [17] characterized the soot collected from a turbocharged GDI (TGDI) and a diesel engine, finding that TGDI soot contains more lubricant oil additive elements and wear metal than diesel soot. Though, the morphology of TGDI and diesel exhaust soot were similar.

Lubricant oil related phenomena, such as fuel - oil dilution and oil - flame interaction, play an important role in the development of new engine concepts and possibly limit further improvements of existing technologies like high pressure gasoline direct injection and downsizing. In this scenario, a numerical approach could be a suitable method to study the fuel - lubricant oil dilution. Nevertheless, an extensive experimental campaign is less affordable in time and cost perspectives especially for low speed pre - ignition (LSPI), which is a destructive phenomenon, and it possibly may cause severe damages to the experimental apparatus. Su et Al. [18] investigated the influence of different injection strategies on the wall film generation and on the soot emission. They found that multiple injections helped to reduce the fuel interaction with the walls, leading to less wall impingement with respect to single injections, thus preventing soot formation and the fuel - lubricant oil interaction. The benefits of the injection split were studied also by Küpper et Al. [19]. In their work, they analyzed by means of experiments and three - dimensional Computational Fluid Dynamics (3D CFD) simulations, the wall film generated with different injection strategies (i.e. single, multiple and late injections) by three biofuels (E0, E20, E85), in a TGDI engine under cold start conditions. The fuels E0 and E20 showed a similar lubricant oil dilution behavior, although the fuel mass in oil with E20 was slightly smaller because of the E20 beneficial vaporization properties. With regards of the E85, the fuel mass in lubricant oil was almost three times higher compared to E0 and E20 under the same injection strategy. However, it was reduced significantly using a triple injection against a double injection.

A critical and comprehensive review of the interactions between lubricant oil and fuel was performed by Taylor [20]. In this work, the Author analyzed the main causes and drawbacks of the

fuel impingement and the lubricant oil dilution by addressing the influence of temperature and dilution level on liquids selected key properties (such as fuel and lubricant oil mixture viscosity, fuel boiling point). Also, he reported the results of experiments performed in passengers' vehicles, which showed the influence of the particulate filter regeneration strategy on the fuel dilution level.

In this context, this work aims to further develop a one - dimensional code, presented in the work [21] and based on the mathematical model of Zhang et Al. [22]. The code, which is updated to Python 3.7, models the contamination of the lubricant oil due to the fuel impingement and allows to estimate the lubricant oil properties degradation and the quality of the lubricant oil - fuel mixture on the cylinder liner wall at the piston arrival, during the compression stroke, in a TGDI engine. Thus, the code is capable to predict the thickening of the thin lubricant oil layer and the amount of the lubricant oil scraped by the piston. To account for PM formation phenomena, the model needs to address the fuel - wall interaction mechanism. In the last code version [21], a fuel layer of given thickness was placed upon the oil layer as initial condition. This was possible because the model worked in an operative condition which promoted LSPI, thus in - cylinder pressure was high, and the start of injection could be assumed to be almost coincident with the end of the injection. Though, in a PM enhancing operative condition (for instance, catalyst heating operation) and in a split injection strategy, the injection and the fuel impingement dynamics need to be accounted for. In this case, being engine load (thus the ambient pressure) lower with respect to a LSPI favorable condition, the mixture formation is more dependent on the fuel spray momentum and the spray penetration is deeper, possibly leading to further fuel wall impact. With these regards, the model is updated to resolve fuel impingement by taking as boundary condition the results of a CFD 3D spray simulation, which gives droplets characteristics and wall impingement rate against time. The model is a fast tool that allows to estimate the influence of several operative parameters (coolant temperature, injection timing etc.) and engine configurations on the interaction of the lubricant oil and the impinged fuel, and to support the definition of spray pattern and fuel/oil properties. After the description of the physical models and some operative considerations, the results of the simulations will be showed and discussed. In particular, the code in this work is adopted to study the dilution of the lubricant oil in a cold start like engine operative point, which is a critical condition for PM formation.

2. Methodology

In this paper, the Authors propose a numerical modelling of the interaction between the lubricant oil and the liquid fuel on the liner wall of an automotive TGDI engine. The code is a further development of a previous version [21]. In particular, the development regards the fuel film formation that is derived from a CFD 3D simulation and whose characteristics will be described later.

To achieve a suitable representation of the physical phenomena observed between the solid wall, the liquid film, and the gaseous phase the model needs to account for i) the heat transfer between the solid wall and the liquid film, ii) the mass and heat transfer between the two liquid phases and iii) the fuel evaporation through a variable grid size. The computational domain is composed by a solid wall, separated by the liquid layer (lubricant oil plus the impinged fuel) by a solid - liquid interface (SLI) and a moving boundary (liquid - gas interface, LGI) to resolve fuel evaporation. After some testing, the solid wall height has been reduced with respect to the real dimension of engine cylinder liner in order to save computational time and to allow faster simulations, since temperature was not varying beyond a certain coordinate, thus not affecting heat transfer. The discretization of the computational domain (Figure 1) is performed by a one - dimensional (1D) approach (along the radial dimension).

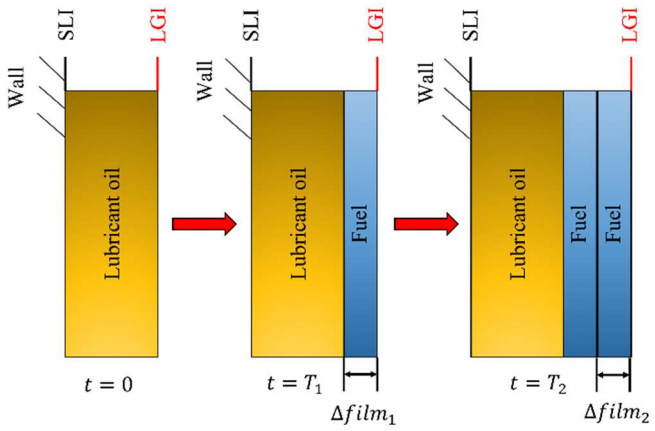

Figure 1. Schematic representation of the computational domain and of the fuel deposition.

2.1. Reference conditions and 1D dilution model workflow

The engine geometrical data and the operative conditions in the present work are listed in table 2 and based on the TGDI research engine of the paper [23]. The operative parameters are selected to simulate a cold start condition, which is critical for soot formation and lubricant oil dilution. With these regards, engine speed is set at 1600 rpm with the intake manifold pressure at 82 kPa and air temperature 20 °C. Engine walls and coolant temperatures are maintained at 30 °C. The same condition is tested with a commercial RON93 gasoline and with a renewable fuel, namely pure iso - octane, which is assumed to be obtained from renewable process involving the use of hydrogen. A fuel mass of 27.8 mg is injected. The injection pressure and the SOI are set to 300 bar and 275 CAD BTDC. The lubricant oil is modelled with a SAE 5W - 30 synthetic oil and its properties are simulated through SimscapeTM Thermal liquid block [24]. The lubricant oil layer is assumed to be constant between the two cases and equal to 4 μm, while the fuel impingement depends on the fuel itself and is given as an output from the CFD 3D simulations. A tuned in - house developed zero - dimensional (0D) engine thermodynamic model provides the necessary initial and boundary conditions for the dilution 1D simulation, i.e. pressure and temperature in the combustion chamber. This 0D model evaluates the in - cylinder temperature and pressure by means of the solution of the internal energy balance and through the perfect gas law, respectively. The 1D dilution simulations angular range goes from the start of injection, when only the thin lubricant oil layer adheres to the cylinder liner, to the instant when the piston scrapes the liquid film, which is the latest available spot for lubricant oil - fuel dilution and for fuel evaporation.

Table 1. Specifications of the single - cylinder research engine and operative conditions.

Parameters	Specifications
Displacement	500 cm^3
Bore x Stroke	86 mm x 86 mm
Geometric Compression Ratio	9.5:1
Engine speed	1600 rpm
Average intake manifold pressure	82 kPa
Intake air temperature	20 °C
Coolant temperature	30 °C

The workflow to provide the necessary initial and boundary conditions to the 1D dilution model and how the code provides its outputs is showed in figure 2. The engine geometry and the operative

conditions are passed to the 0D engine model, the CFD 3D software and directly to the 1D dilution model. Then, the 0D engine model provides the time dependent in - cylinder temperature and pressure to both the dilution model and the CFD 3D software. Then, CFD 3D simulations are performed to account for droplets impingement on the liner surface. Thus, the droplets data and the impact time information are uploaded into the 1D dilution model, which simulates the lubricant oil - fuel film formation, the heat and mass transfer phenomena and the fuel evaporation.

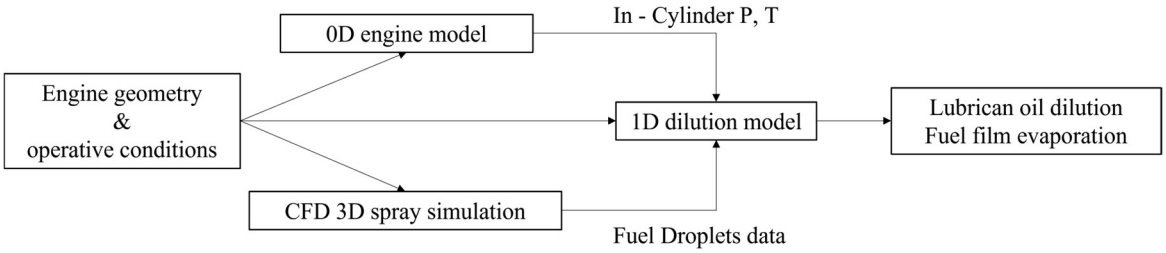

Figure 2. Schematic representation of the adopted workflow. The code main inputs and outputs are showed.

2.2. Fuel film deposition strategy and numerical stability

In the framework of oil - fuel simulations, especially in the case of split injection strategy, the 1D code needs to be provided with size and velocity of the impacting fuel droplets during the injection simulation time. Those droplet data were defined by means of CFD spray simulations performed with the STAR - CD v4.28 commercial software. The CFD simulations were conducted in a quiescent vessel box with dimension 86 x 86 x 50 mm chosen in order to emulate the free - path available for the liquid fuel spray in the volume enclosed by the stroke x bore reference engine. The injection point was placed at the external boundary of the box in order to emulate a wide spacing injector configuration. The vessel was meshed with hexahedral cells of 0.8 mm which fine up to 0.4 mm 5 mm around the injector point in order to capture the spray breakup at the nozzle exit with increased accuracy. The RANS two - equations RNG k - ε model was adopted for the turbulence whilst a tuned version of the model by Brusiani et al. [25] was used for the spray breakup. Second order schemes were used for the transport equations, and the time-step was set to $1 * 10^{-6}$ s. In order to reproduce the spray impact characteristics under catalyst heating-like conditions, the air pressure and temperature in the environment were set to 0.82 bar and 20 °C whilst a fixed temperature of 30 °C was adopted at the walls.

With regards to the injection setting, the features of the Bosch HDEV5 multi - hole GDI injector from [26] were considered as representative of nowadays injection systems. The main injector data used in the simulation are listed in table 2. It is underlined that for the sake of simplicity, the CFD simulations were performed considering a single jet, whose droplets' data (velocity, diameter) were recorded and averaged in the layer of cells upon the impact wall. For the sake of clarity, the CFD domain is shown in figure 3.

Table 2. Injector data.

Injector	Multi-hole Bosch HDEV5
Spray type	Full cone
Jet cone angle	16 °
Nozzle minimum diameter	210 μm
HFR @100 bar with n-heptane	20 cc/s

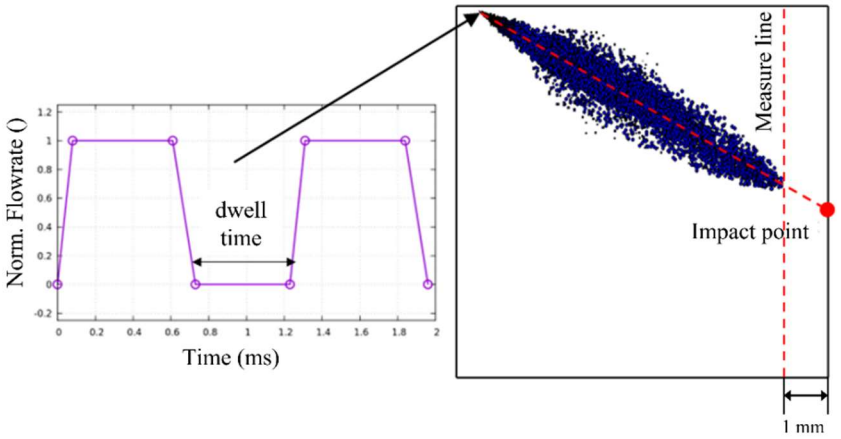

Figure 3. Injection profile over time (left) and representation of the CFD domain with fuel droplets (right).

The 1D dilution model acquires the mean droplets diameter and the mean velocity for each CFD time step. Droplets data, in the CFD simulation, are stored when the droplets cross the lateral surface of a control volume, represented in figure 3 with the red dashed line and identified as the measure line. This surface is 1 mm distant and parallel to the face (as shown in figure 3) of the vessel box subjected to fuel impact. The 1D code, assuming the spray breakup phase to be already completed and that the droplets velocity keeps constant, needs to calculate the time for the droplet to cover the free - path distance from the measure line to the wall by means of the droplets' velocity ($v_{droplet}$). This time is then converted into 1D model iterations ($n_{iteration}$) by dividing for the 1D model time step (dt_{1D}), as shown in equation (1). Figure 4 (a) shows the actual droplets wall impact frequency and the normalized flowrate against time once the droplets impact delay, due to the distance between the injector tip and the wall is accounted for. Figure 4 (b) shows the droplets diameter and velocity evolution against time. At this point, the 1D code takes the impact frequency and the droplets data as boundary conditions and accounts for the droplets' deposition on the lubricant oil layer, increasing the total film height. Also, the 1D model accounts for the fuel deposition and the dilution of a representative point of the total area exposed to fuel impingement.

$$n_{iteration} = \frac{1x10^{-3}}{v_{droplet} \cdot dt_{1D}} \tag{1}$$

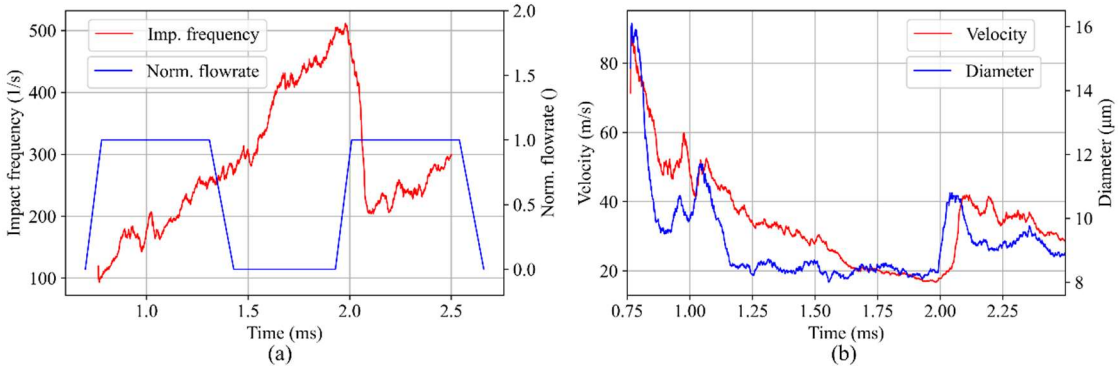

Figure 4. Results of the CFD 3D simulation: (a) droplets impact frequency (red) and normalized flowrate (blue) against simulation time, (b) droplets velocity (red) and diameter (blue) against simulation time (right).

The code accounts for the droplet deposition by calculating the spread diameter for each droplet: the droplets characteristic Weber number lies in the spread/splash regime, but splashing phenomenon is not accounted for. The spread mechanism is schematised in figure 5. The mean spread diameter (D_S) is calculated with equation (2) [27], once the mean diameter (d), the mean velocity and the Weber number (We) are known (k_1 and k_2 are constants).

$$D_S = k_1 \cdot d \cdot We^{k_2} \tag{2}$$

Then, the film height increment ($h_{d,i}$) is evaluated by means of the cell area and the mass conservation law at each time step and for each droplet: when the cumulative increment reaches the base grid size, which is 0.1 μm, a new fuel cell is added to the computational domain.

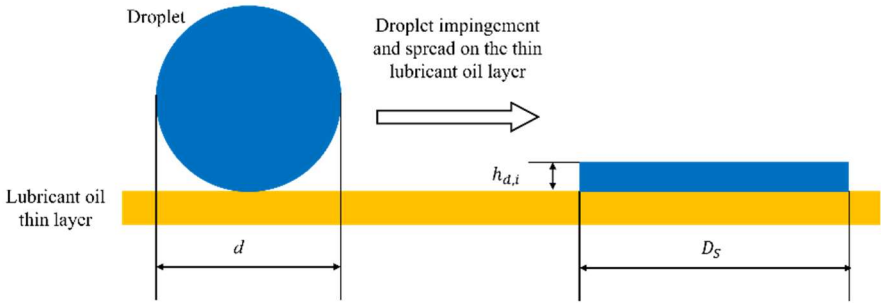

Figure 5. Schematization of a fuel droplet impacting and spreading into the lubricant oil layer.

The 1D model base grid size is set up and optimized after numerical stability and computational time considerations, assuming that the liquid phase diffusion phenomena occur in a height of dozens of microns. With these regards, the model time step is calculated according to the Courant - Friedrichs - Lewy (CFL) condition for thermal diffusion once the base grid size is known. For this reason, the Authors implemented a variable grid size and established an inferior limit to the base grid size to account for fuel evaporation without incurring in numerical instability or excessive computational cost and to prevent the instantaneous removal of liquid cells.

As previously mentioned, the model needs to account for mass and heat transfer and for fuel evaporation: the next subsection briefly describes the adopted methodology, while a more comprehensive and detailed description of the model equations, the boundary conditions and the variable grid size can be found in the work [21].

2.3. Film dilution and fuel evaporation

The heat transfer is governed by a 1D Fourier's equation (equation (3)) for both the solid and the liquid phases, being α the thermal diffusion coefficient. The coolant - side temperature is assumed to hold constant and equal to the coolant temperature because of the absence of heat sources and the high thermal capacity of the coolant, while the gas side temperature is derived from an in - house developed 0D model and cooled by the fuel evaporation. The heat transfer coefficient (HTC) is provided by the Woschni's correlation [28] that is defined through some coefficients (C_1 and C_2), which depend on the engine stroke. A Robin boundary condition (BC) is adopted at the liquid - gas interface, being the difference between the liquid film temperature ($T_L|_{LGI}$) and the free stream temperature (T_∞) the driver for heat transfer, as equation (4) shows. The free stream temperature is the gas temperature reduced by the cooling effect of the fuel evaporation.

The second Fick's diffusion law (equation (5)) models the mass transfer between the lubricant oil and the fuel under the assumptions of i) thin liquid film, ii) no viscous dissipations, iii) lubricant oil -

fuel dilute mixture and iv) pseudo - pure liquids. The liquid phase diffusion coefficient (D_L) is estimated through the empirical correlation of Siddiqi and Lucas [29]. At the SLI a no slip and no penetration condition are implemented, while convective mass transfer is evaluated by means of equation (6).

$$\frac{dT}{dt} = \alpha \frac{d^2T}{dx^2} \tag{3}$$

$$k_L \frac{dT_L}{dx}\bigg|_{LGI} = HTC \cdot (T_L|_{LGI} - T_\infty) \tag{4}$$

$$\frac{d\xi}{dt} = D_L \frac{d^2\xi}{dx^2} \tag{5}$$

$$D_L \frac{d\xi_F}{dx}\bigg|_{LGI} = MTC \cdot \xi_F\big|_{LGI} = \dot{m} \tag{6}$$

Finally, the liquid film height is updated once the liquid height in the last iteration step (h_{i-1}) and the fuel mass evaporation rate $\dot{m}$ are known.

3. Results

In this section the simulation results from the 1D model are reported. The engine main features and the main operative parameters are listed in table 1. This set up aims to reproduce a cold start engine condition to address the most critical phase for PM formation and understand how cylinder liner fuel impingement affects the lubricant oil layer properties, in particular dynamic viscosity. With these regards, the dilution of a SAE 5W - 30 lubricant oil is tested with two different fuels, a four-component RON93 surrogate (40.7 mol% i - octane, 13 mol% n - heptane, 40.7 mol% toluene, 5.7 mol% 1 - pentene) from [30] and pure iso - octane. The 1D simulations start at the SOI, while they end when the piston reaches the liquid film and scrapes it: in this study, being the spray targeting angle of 30 ° with respect to a normal plane to the cylinder axis, being the engine square and considering the centre of the area of the droplets impact, the liquid film lies at half of the engine stroke. This means that 1D the simulations end at half of the compression stroke, i.e. at 630 CAD. In figure 6 are presented the fuel concentrations at different distances from the liner wall and the film thickness evolution in time. As long as the injected mass is the same for both the study cases, the fuel film thickness depends on the fuels' densities: being the cells volume fixed, the lower iso - octane density (≈ 9 % less with respect to the RON93) leads to a maximum film height which is approximately 27 % lower in comparison with the one resulting from the RON93 case. The maximum film heights are ≈ 69 μm and ≈ 94 μm for the iso - octane and RON93 cases respectively. Evaporation trends are similar: the low in - cylinder and wall temperatures and the in - cylinder pressure, which are typical for a cold start and a catalyst heating conditions, results in a low HTC, a low MTC and finally a low fuel evaporation rate. It must be specified that oil evaporation is not considered because the engine is not firing and the simulation temperatures, typical for a motored operative condition, does not enable lubricant oil evaporation. The lubricant oil layer viscosity reduction, the in - cylinder temperature and the concentration difference reduction affect the liquid phase diffusion coefficient leading to a smoother liquid phase dilution in the second half of the simulation.

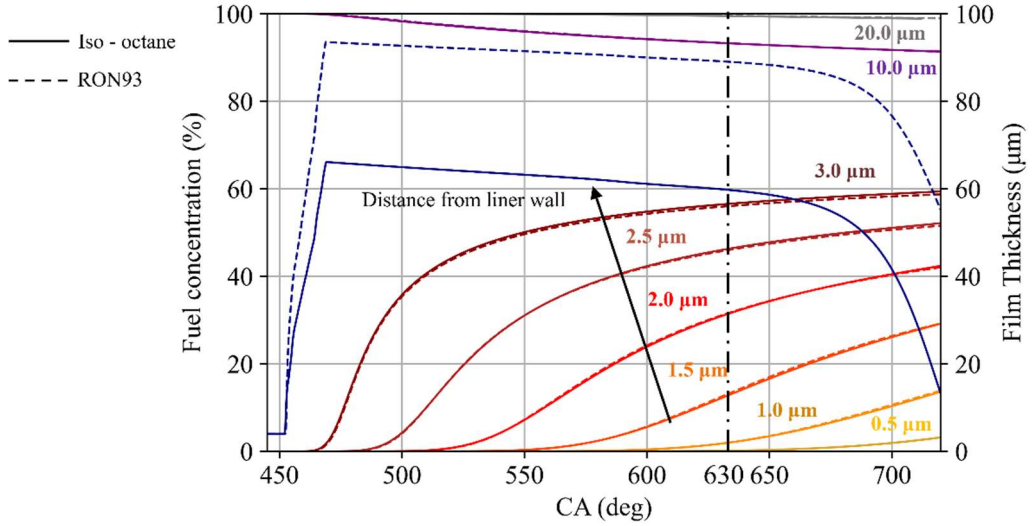

Figure 6. Film thickness and fuel concentration evolution during the 1D simulation at different distances from the liner wall: solid line is iso - octane and dashed line is RON93.

Figure 7 shows the viscosity and the fuel fraction time - evolution in the film height that goes from the liner wall (distance of 0 µm from cylinder liner wall) to the last lubricant oil cell at simulation start (distance of 4 µm) and that is referred to as the "oil side". In the presented model lubricant oil viscosity degradation directly depends only on fuel and oil mass fraction: film viscosity, thermal conductivity, specific heat and density are evaluated only at the initial conditions of temperature and pressure. As the fuel droplets impact the lubricant oil layer, they start to dilute the wall film, leading to a fast viscosity degradation. As long as the simulation continues, the dilution process slows down because the concentration gradients between cells decrease and the fuel fraction and the film viscosity curves tend to flatten.

Figure 8 shows the lubricant oil mass fraction percentages, with respect to the total lubricant oil mass, in the liquid film region comprised from 4 µm (distance from liner wall) and the LGI, which is referred to as the "fuel side", and the film thickness reduction percentages due to fuel evaporation. The liquid phase diffusion coefficient depends also on liquid phases' molar volume, density and temperature, thus on the fuel type. This leads to the transfer of ≈ 30 % of the total lubricant oil mass from the "oil side" to the "fuel side" for both the iso - octane and the RON93 cases at 630 CA. Film evaporation trend is comparable in the two study cases: though, given the different maximum film height reached in the two simulations due to the different fuel density of the tested fuels, a residual film length of ≈ 60 µm for the iso - octane and ≈ 90 µm for the RON93 is achieved, resulting in a residual liquid phase is the ≈ 90 % and the ≈ 95 % (against the maximum film length) for the iso - octane the RON93 respectively. This means that the piston would scrape a film height of ≈ 56 µm and ≈ 86 µm in the two cases.

These results show that, in a motored engine condition, the impinged fuel on the cylinder liner wall dilutes the lubricant oil reducing the oil layer viscosity. Small differences are captured between the effects of the two different tested fuels on the oil dilution and viscosity reduction, while the film maximum height is strictly dependent on the fuel density, once the same fuel mass is injected. Thus, for both cases the lubricant oil mass fraction scraped by the piston in the compression stroke is not negligible, leading to a strong lubricant oil mass loss and possibly to the scattering of lubricant oil particles in a cold start operative condition in a TGDI engine. Also, the oil viscosity degradation could lead to engine moving parts wear.

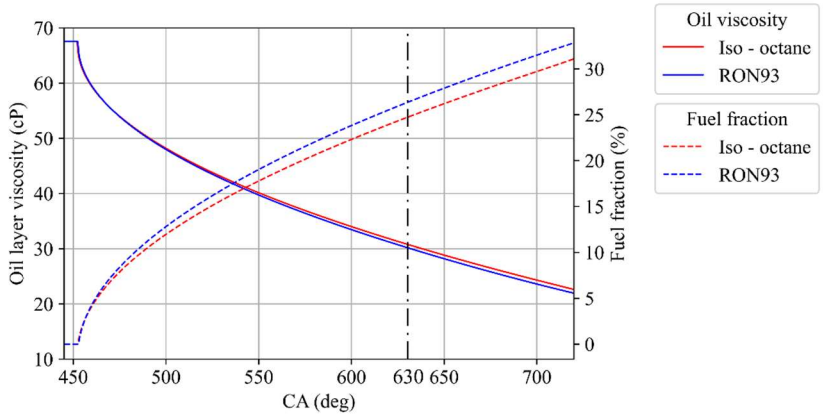

Figure 7. Oil viscosity degradation and fuel fraction in the thin lubricant oil layer during the 1D simulation.

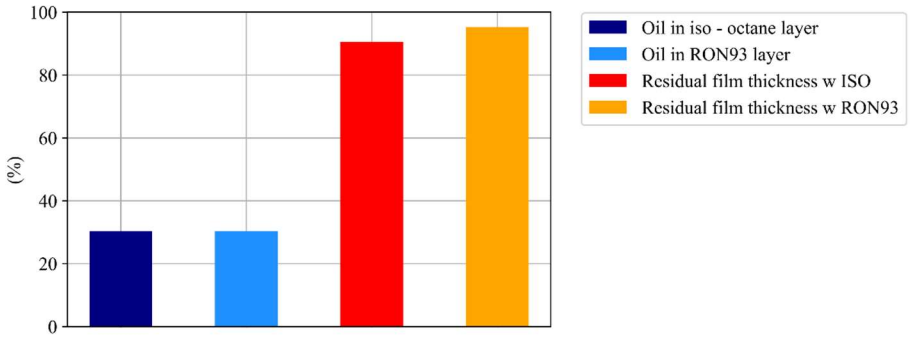

Figure 8. Lubricant oil mass fraction in the film that goes from 4 μm to the right end of the film with respect to the total lubricant oil mass, and the film thickness reduction due to fuel evaporation.

4. Conclusion

This paper addresses, by means of a one - dimensional modelling, the interaction between lubricant oil and impinging fuel under relevant TGDI operative conditions for particulate matter formation, i.e. engine cold start or catalyst heating operations. Three dimensional CFD simulations are performed to achieve droplets impact data, which are introduced into the 1D model to evaluate the lubricant oil contamination and the fuel evaporation. Two different fuels are tested, then the simulation results are presented and compared. The 1D dilution model proved to be capable to qualitatively predict the lubricant oil - fuel dilution and the fuel evaporation once the fuel droplets impact on the thin lubricant oil layer on a cylinder wall liner due to the injection event. The simulations results show that fuel - lubricant oil dilution strongly reduces the lubricant oil viscosity and leads to a lubricant loss of ≈ 30 % of the initial lubricant oil mass for both the tested fuels. The code can also provide insights on the injection pattern and timing influence on the interaction between lubricant oil and fuels, both synthetic and traditional gasolines. In a future perspective, engine fuelled with pure iso – octane, for instance obtained from renewable sources, could suffer of lubricant oil viscosity reduction and oil mass losses. In general, the code could be a useful tool to evaluate e - fuels wall impingement effect on the lubricant oil layer. With these regards, since e - fuels properties are known the model accuracy is improved. Also, PM from lubricant oil has been found in hydrogen and natural gas - powered engines, rising lubricant oil related phenomena interest. In this context, the code could be a useful tool to study and compare the effect of different injection strategies on the wall impingement and on the lubricant oil dilution under relevant engine operative condition, with traditional and innovative fuels.

References

[1] Raza M, Chen L, Leach F and Ding S 2018 Energies 11.
[2] Wang C, Xu H, Herreros, J M, Wang J and Cracknell R 2014 App. Energy 132 178-91.
[3] Jing D, Zhao H, Li Y, Guo H, Xiao J and Shuai S J 2018 SAE Tech. Paper.
[4] Zhang W, Ma X, Xinhui L, Shuai S, Wu K, Macias J, Shen Y, Yang C and Guan L 2020 SAE Technical Paper.
[5] Voice A, Singh R, Levy R and Fatouraie M 2021 SAE Int. J. Advances & Curr. Prac. in Mobility.
[6] Mahmud R, Kurisu T, Akgol O, Nishida K and Ogata 2020 SAE Int. J. Advances & Curr. Prac. in Mobility.
[7] Chung J, Kim N, Choi H and Min K 2016 SAE Tech. Paper Series SAE Int.
[8] Shanta S M, Molina G J and Soloiu V 2011 Adv. in Tribology 1-7.
[9] Cousseau T, Acero J S R and Sinatora A 2016 Tribology Int. 100 60-9.
[10] Dahnz C, Spicher U and Arcoumanis D 2010 Int. J. of Engine Research 11 485-98.
[11] Palaveev S, Magar M, Kubach H, Schiessl R, Spicher U and Maas U 2013 SAE Int. J. of Engines 6 54-66.
[12] Luo X, Teng H, Hu T, Miao R and Cao L 2015 SAE Int. J. of Engines 8 520-8.
[13] Yi H, Seo J, Yu Y S, Lim Y, Lee S, Lee J, Song H and Park S 2022 Sci. Rep. 12.
[14] Amirante R, Distaso E, Napolitano M, Tamburrano P, Iorio S D, Sementa P and Reitz R D 2017 Int. J. Of Engine Research 18 606-20.
[15] Miller A L, Stipe C B, Habjan M C and Ahlstrand G G 2007 Environ. Sci. Technol. 41 6828-35.
[16] Pfau S A, Rocca A L, Haffner-Staton E, Rance G A, Fay M W and McGhee M 2019 SAE Tech. Paper Series.
[17] Uy D, Ford M A, Jayne D T, O'Neill A E, Haack L P, Hangas J, Jagner M J, Sammut A and Gangopadhyay A K 2014 Tribology Int. 80 198-209.
[18] Su J, Xu M, Yin P, Gao Y and Hung D 2014 SAE Int. J. of Engines 8 20-29.
[19] Küpper C, Artmann C, Pischinger S and Rabl H P 2014 Auto Tech Review 3 30-35.
[20] Taylor R I 2021 Lubricants 9 92.
[21] Mariani V, Bianchi G M, Cazzoli G and Falfari S 2020 E3S Web of Conferences 197.
[22] Zhang Q, Kalva V T and Tian T 2018 SAE Tech. Paper Series.
[23] Kim N, Chung J, Kim J, Cho S and Min K 2022 Energy Conv. and Man. 252.
[24] MATLAB and Simscape Toolbox Release 2020a, The MathWorks, Inc., Massachusetts, United States.
[25] Brusiani F, Bianchi G M and Tiberi A 2012 SAE Tech. Paper Series.
[26] Schulz F, Samenfink W, Schmidt J and Beyrau F 2016 Fuel 172 284-92.
[27] Eckhause J E and Reitz R D 1995 Atomization and Sprays 5 213-42.
[28] Woschni, G. A SAE Tech. Paper Series.
[29] Siddiqi M A and Lucas K 1986 The Canadian J. of Chem. Engineering 64 839-43.
[30] Piehl J A, Zyada A, Bravo L and Samimi-Abianeh O 2018 J. of Combustion 1-27.